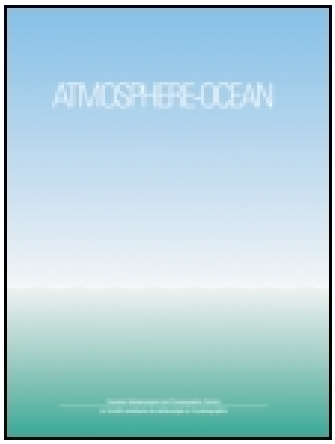

Atmosphere-Ocean
Publication details, including instructions for authors and subscription information:
http://www.tandfonline.com/loi/tato20

Testing and Modelling the Volatility Change in ENSO

R. Modarres[a] & T. B. M. J. Ouarda[ab]

[a] Hydroclimate Modelling Group, INRS-ETE, 490 De La Couronne, Québec, Quebec, Canada

[b] Institute Center for Water Advanced Technology and Environmental Research (iWATER), Masdar Institute of Science and Technology, P.O. Box 54224, Abu Dhabi, United Arab Emirates

Published online: 07 Oct 2013.

To cite this article: R. Modarres & T. B. M. J. Ouarda (2013) Testing and Modelling the Volatility Change in ENSO, Atmosphere-Ocean, 51:5, 561-570, DOI: 10.1080/07055900.2013.843054

To link to this article: http://dx.doi.org/10.1080/07055900.2013.843054

Testing and Modelling the Volatility Change in ENSO

R. Modarres[1,*] and T. B. M. J. Ouarda[1,2]

[1]*Hydroclimate Modelling Group, INRS-ETE, 490 De La Couronne, Québec, Quebec, Canada*
[2]*Institute Center for Water Advanced Technology and Environmental Research (iWATER), Masdar Institute of Science and Technology, P.O. Box 54224, Abu Dhabi, United Arab Emirates*

[Original manuscript received 27 May 2013; accepted 31 July 2013]

ABSTRACT *The El Niño–Southern Oscillation (ENSO) is by far the most energetic climate signal. Any change in ENSO characteristics will have serious consequences for the global climate system. This work suggests a different view at the change in ENSO volatility in addition to change in its descriptive statistics. The volatility or the conditional variance of ENSO is tested and modelled using both the Autoregressive Moving Average–Generalized Autoregressive Conditional Heteroscedasticity (ARMA-GARCH) error model and the GARCH model, to investigate the change in the short-run and long-run persistency of the second-order moment of ENSO before and after a change point detected by a Bayesian change point analysis. Nonparametric tests revealed a significant change in descriptive statistical characteristics such as the mean, the (unconditional) variance, and the probability distribution of ENSO after a change point in 1975. An Engle's test did not show heteroscedasticity in the random process (residuals) of the Southern Oscillation Index (SOI) time series before 1975 although heteroscedasticity increased and appeared after 1975. The GARCH model indicates an increasing short-run persistency after 1975 and decreasing long-run persistency. A seasonal shift in extreme heteroscedasticity is observed from summer to winter. In addition, the non-linearity and nonstationarity of the SOI volatility have increased in recent decades. This may be caused by an increase in frequency and magnitude of extreme volatilities after 1975. The results of this study indicate that ENSO has become more dynamic and uncertain in recent decades. The increase in the frequency of extreme events together with extreme conditional variance after 1975 may increase the prediction uncertainty of ENSO-driven climate phenomena.*

RÉSUMÉ *[Traduit par la rédaction] Le El Niño–oscillation australe (ENSO) est de loin le signal climatique le plus énergétique. Tout changement dans les caractéristiques de l'ENSO aura de sérieuses conséquences sur le système climatique planétaire. Le présent travail propose un regard différent sur le changement dans la volatilité de l'ENSO en plus du changement dans ses statistiques descriptives. Nous testons et modélisons la volatilité ou variance conditionnelle de l'ENSO en nous servant à la fois du modèle d'erreur ARMA–GARCH (moyenne mobile autorégressive – hétéroscédasticité conditionnelle autorégressive généralisée) et du modèle GARCH pour étudier le changement à court terme et à long terme de la persistance du moment de second ordre de l'ENSO avant et après un point de changement détecté par une analyse bayésienne de point de changement. Des tests non paramétriques ont révélé un changement significatif dans les caractéristiques statistiques descriptives comme la moyenne, la variance (inconditionnelle) et la distribution de probabilités de l'ENSO après un point de changement en 1975. Un test d'Engle n'a pas montré d'hétéroscédasticité dans le processus aléatoire (résidus) de la série chronologique de l'indice d'oscillation australe (SOI) avant 1975, bien que l'hétéroscédasticité ait augmenté et soit apparue après 1975. Le modèle GARCH indique une persistance à court terme croissante après 1975 et une persistance à long terme décroissante. Nous observons un déplacement saisonnier dans l'hétéroscédasticité extrême de l'été à l'hiver. De plus, le caractère non linéaire et non permanent de la volatilité du SOI s'est accentué au cours des dernières décennies. Cela peut être dû à un accroissement dans la fréquence et l'amplitude des volatilités extrêmes après 1975. Les résultats de cette étude indiquent que l'ENSO est devenu plus dynamique et plus incertain au cours des dernières décennies. L'accroissement dans la fréquence des événements extrêmes de pair avec la variance conditionnelle extrême après 1975 peut augmenter l'incertitude prévisionnelle des phénomènes climatiques liés à l'ENSO.*

KEYWORDS SOI; GARCH; volatility; climate change; conditional variance; Bayesian change point detection

1 Introduction

The El Niño–Southern Oscillation (ENSO) phenomenon is a strong climate-dominant mode in the Pacific which has major effects on the global climate system and ecosystem as well as significant socio-economic consequences around the globe (e.g., Chen, McCarl, & Hill, 2002; Ropelewski &

*Corresponding author's email: Reza.Modarres@ete.inrs.ca

Halpert, 1987; Shabbar & Khandekar, 1996). Therefore, any change in ENSO characteristics and ENSO variations in the past, present, and future has been a topic of interest in recent decades. Many studies have reported changes in ENSO characteristics. For example, it is reported that the change in the statistical moments of ENSO is an important indicator of human-induced climate change (Timmermann, 1999). The period and growth rate of ENSO can also be affected by the strength of ocean–atmosphere feedbacks (Wang, 2007). Over the last century, ENSO characteristics underwent significant changes (An & Wang, 2000). Qian, Wu, Congbin, and Wang (2011) applied an empirical mode decomposition (EMD) method to investigate changes in the frequency of ENSO that indicated a 30% increase in amplitude of the ENSO interannual variability around 1937. More recently, Wu, Huang, Long, and Peng (2007) also showed a change in ENSO using an EMD method.

Non-linearity is an important aspect of ENSO characteristics. The non-linearity of ENSO is important because, as a global climate-driving phenomenon, any change in the non-linearity of ENSO may have unpredictable and complex influences on the global atmospheric cycle. Different studies have investigated non-linearities in the ENSO cycle from different points of view (e.g., Boucharel et al., 2011; Hall, Skalin, & Teresavirta, 2001; Philip & van Oldenborgh, 2009) and have discussed the factors influencing the non-linearity of ENSO.

Although changes in the statistical properties of ENSO have been examined, very few studies have paid attention to the second-order moment or the variance of ENSO. For example, Cobb et al. (2013) showed that ENSO variance in the twentieth century is significantly higher than ENSO variance in the average fossil coral record. Xue, Smith, and Reynolds (2003) showed the interdecadal change in the standard deviation (SD) of sea surface temperature (SST) normals. Stahle et al. (1998) showed the long-term heteroscedasticty (conditional variance) in the reconstructed winter Southern Oscillation Index (SOI). Chu, McAleer, and Chen (2012) also investigated the conditional variance of ENSO and its change in recent decades from 1933 to 2007.

The present study proposes to look at the change in ENSO through the change in its time-varying second-order moment, the conditional variance, or the heteroscedasticity of ENSO using the Generalized Autoregressive Conditional Heteroscedasticity (GARCH) model. The Bayesian change point detection method is also used, which is based on the highest probability of change occurrence in a time series from the posterior distribution.

The investigation of this change point and volatility change is carried out using SOI time series for 1940–2011 (Fig. 1) calculated from the monthly or seasonal fluctuations in the air pressure between Tahiti and Darwin obtained from the National Weather Service (NOAA, 2012).

This time period was chosen to investigate and highlight the changes in the statistical and stochastic characteristics and the volatility of ENSO during recent decades and to illustrate the usefulness of the proposed method for investigating ENSO volatility change.

2 Methodology

a *GARCH Modelling of SOI Time Series*

Using SOI time series with the following mean process

$$\mathrm{SOI}_t = \mu + \varepsilon_t \quad \varepsilon_t \sim \mathrm{N}(0, \sigma_t^2), \tag{1}$$

where the residuals ε_t have a normal distribution with variance $\sigma_{\varepsilon_t}^2$.

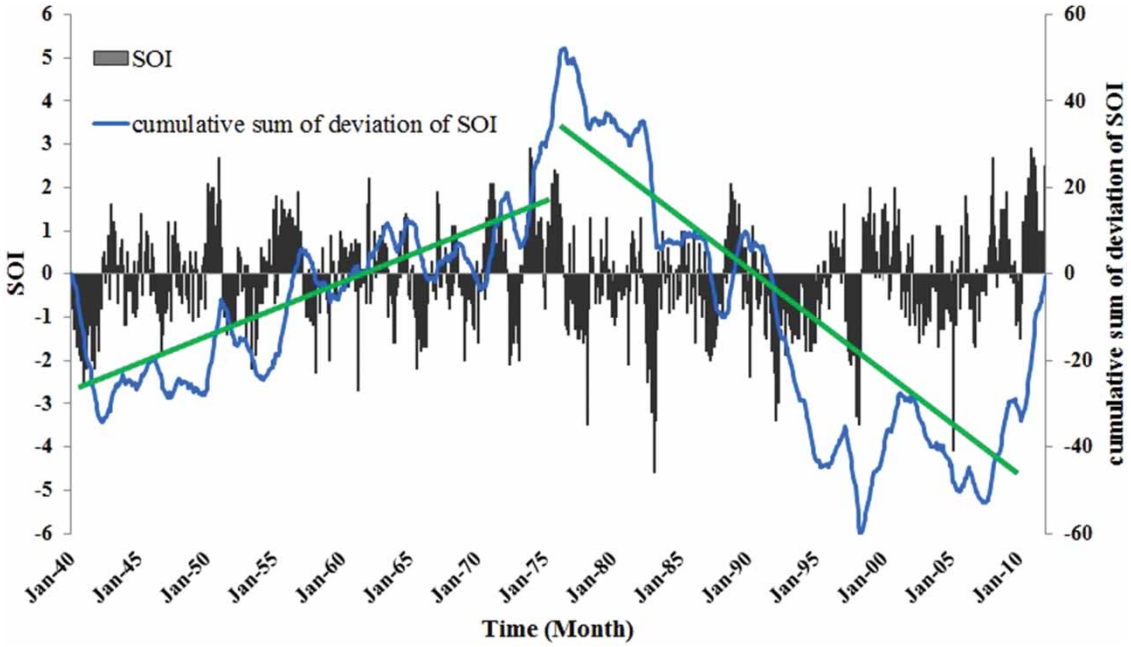

Fig. 1 Illustration of Bayesian change point detection analysis for the SOI time series (1940–2011). The green lines show the trend in the cumulative sum of the deviation of SOI before and after 1975.

We can capture the dynamic characteristics of the mean, μ, by an Autoregressive Moving Average (ARMA) model. The ARMA(p, q) model for the SOI time series can be written as follows:

$$\varphi_p(B)\mathrm{SOI}_t = \theta_q(B)\varepsilon_t, \tag{2}$$

where $\varphi_p(B)$ is the polynomial of order p, $\theta_q(B)$ is a polynomial of order q, and B is a backward operation. The heteroscedasticity of the residuals, ε_t, of the ARMA model or $\sigma^2_{\varepsilon_t}$, can be modelled using a GARCH approach.

This type of model is called an ARMA-GARCH error model. In this model, the conditional mean of a variable is assumed to follow an ARMA process while the conditional variance remaining in the residuals is modelled using a GARCH approach (Modarres & Ouarda, 2012). It should be noted that there are few studies on the application of the ARMA approach to modelling SOI time series (e.g., Ahn & Kim, 2005; Chu & Katz, 1985; Trenberth & Hoar, 1997). However, these studies did not investigate the change point in the SOI time series or the statistical and stochastic changes before and after the change point.

The volatility or the heteroscedasticity of the time-varying variance of a time series is estimated using a GARCH approach (Bollerslev, 1986). The GARCH is the generalized form of the Autoregressive Conditional Heteroscedasticity (ARCH) model developed by Engle (1982). GARCH(v, m) assumes that the variance or the second-order moment of the time series varies in time and has its own memory of past variances. This model can be specified as follows:

$$\sigma_t^2 = \omega + \sum_{i=1}^{v} \alpha_i \varepsilon_{t-i}^2 + \sum_{j=1}^{m} \beta_j \sigma_{t-j}^2, \tag{3}$$

where ω is a constant, α and β are parameters of the model to be estimated, v and m are the orders of the model, σ_t^2 is the conditional variance at time t, and σ_{t-j}^2 is the conditional variance at time step $t-j$, and ε_{t-i}^2 is the squared residuals at time step $t-i$.

In this model, the short-run persistency in conditional variance is defined by the ARCH parameter (α), and the long-run persistency in conditional variance is defined by the GARCH parameter (β). The high value of $\alpha+\beta$ indicates a high intensity of persistence in the conditional variance of the time series.

To build an ARMA-GARCH model, it is therefore important to first test the existence of the time-varying variance, or the ARCH effect, in the residuals of an ARMA model. The main approach to testing the ARCH effect is Engle's Lagrange Multiplier test (Engle, 1982). The test statistic is given by NR^2, where N is the sample size and R is the sample multiple correlation coefficient computed from the regression of ε_t^2 on a constant and $\varepsilon_{t-1}^2, \ldots \varepsilon_{t-v}^2$. The null hypothesis of no ARCH effect cannot be rejected if the test statistic is asymptotically distributed as a chi-squared distribution with v degrees of freedom. We consider $p = 0.05$ to be the rejection level of the null hypothesis of no ARCH effect in the residuals of an ARMA model.

b *Change Point Detection*

Because of the growing evidence for climate change, change point analysis in hydrologic and climatic time series requires revision using new methods. One of these new methods is Bayesian change point detection (Seidou & Ouarda, 2007). Although classical statistics may give the most probable position of the change point, the advantage of the Bayesian method is that it provides a full posterior probability distribution of its position. By applying Bayesian change point detection, the posterior distribution of probability of the number of changes is estimated first. A number of detected change points with the highest probability of occurrence are then chosen. Then, Bayesian inference provides the time position of each selected change point and its probability distribution of occurrence (for more details see Ehsansazeh, Ouarda, & Saley, 2011). In this study, we apply this method to find any possible change points in the SOI time series in order to compare the statistical and stochastic features of SOI before and after any detected change point.

c *Test Methods for Statistical Comparison*

In order to compare the change in SOI statistical characteristics before and after the change point, three nonparametric tests are used (Conover, 1999): the Wilcoxon test which is a robust test to construct the hypothesis of equality of the mean of two different populations; the Levene test which hypothesizes the equality of two population variances; and the Kolmogorov-Smirnov (KS) test which hypothesizes the equality of cumulative distribution functions (CDFs) of two populations.

Moreover, to test the change in stationarity and non-linearity of the SOI and its heteroscedasticity, the Augmented Dickey Fuller (ADF) test (Dickey & Fuller, 1979) for stationarity and the Brock-Dechert-Scheinkman (BDS) test (Brock, Dechert, Scheinkman, & LeBaron, 1996) for non-linearity are employed. The ADF test is used to test the presence of a unit root in the series based on considering an autoregressive AR(1) model. If the autoregressive parameter is equal to one, the process is considered nonstationary. Otherwise, the process is stationary. The BDS test is useful to detect deterministic chaos based on the correlation integral of the time series and shows the time series dynamic by testing the serial independence and temporal correlation. These two tests are applied to compare the SOI and its volatility before and after the change point. For details of the formulations of these tests see Wang (2006).

3 Results and discussion

a *Bayesian Change Point Detection*

Using the Bayesian change point method, a change point in the SOI time series was detected in 1975. By partitioning the time

Table 1. Descriptive statistics of the SOI time series.

SOI Series	Mean	(Unconditional) Variance	Skewness	Kurtosis	Maximum	Minimum
1940–2011	–0.11	1.18	–0.19	3.54	2.9	–4.6
1940–1975	–0.0014	1.02	0.078	–0.137	2.9	–2.7
1976–2011	–0.22	1.34	–0.31	0.756	2.9	–4.6

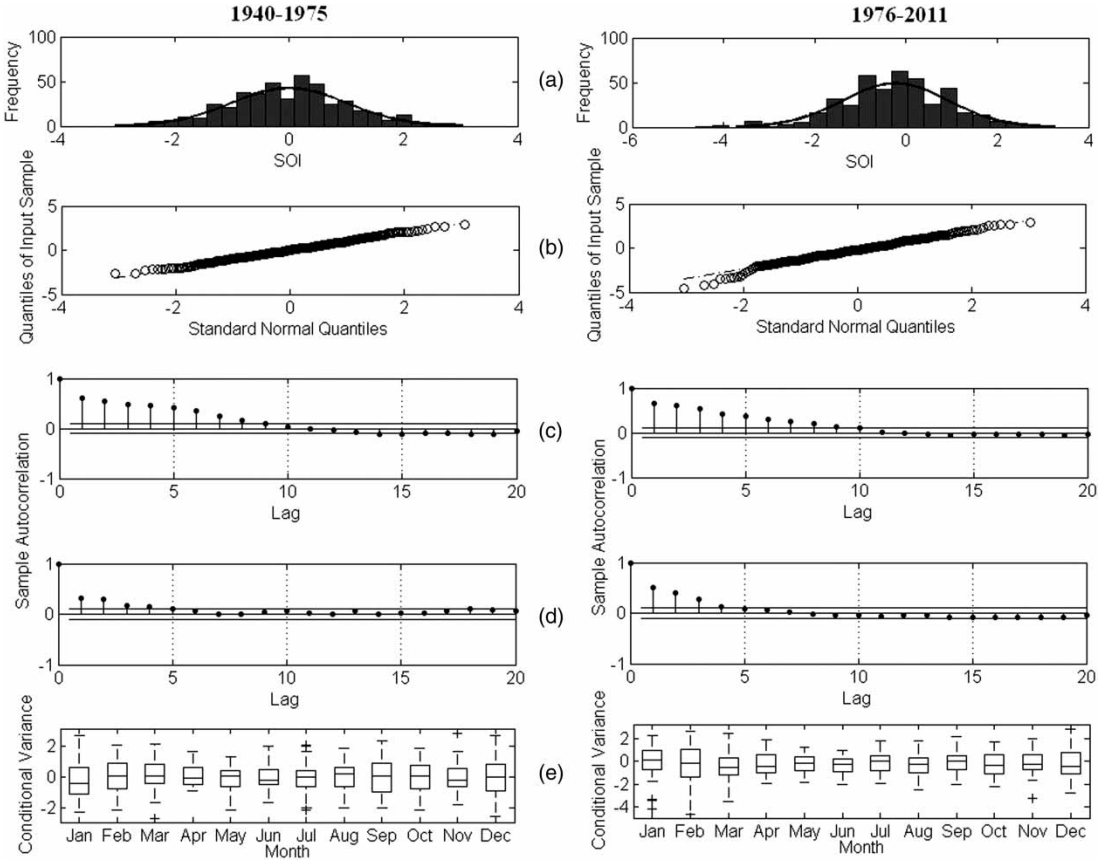

Fig. 2 Exploratory data analysis plot for the SOI time series: (a) normal histogram, (b) quantile-quantile plot, (c) ACF for SOI, (d) ACF for squared SOI, and (e) monthly box plot.

series based on the detected change point and fitting a regression line to each segment (Fig. 1), the SOI is divided into two segments, 1940–75 and 1976–2011. This change point indicates a shift in the trend direction of the SOI time series during the study period. The next step is to compare the statistical and stochastic features, such as the magnitude or frequency of the SOI before and after 1975.

It should be noted that Latif and Keenlyside (2009) also noticed a slight interannual variability during the last century, or the so-called regime shift in the mid-1970s, in the Tropical Pacific climate system based on SST anomalies along the Pacific equator. However, they did not mention the exact timing of the SOI change point. Robbins, Gallagher, Lund, and Aue (2011) detected a change point in 1978 by using SOI time series from 1950 to 1987. However, this change point was reported for the mean (first-order moment of the SOI) but not for the variance of the SOI.

b *Statistical Comparison of the SOI before and after 1975*

Considering 1975 as a change point in the SOI time series, the change in the descriptive statistics of the SOI is first investigated. It can be seen in Table 1 that the descriptive statistics, such as the mean, (unconditional) variance, skewness, and kurtosis, show a remarkable change after 1975. The average SOI changed from zero to –0.22 and the (unconditional) variance of the SOI increased from 1 to 1.3. Moreover, the distribution of the SOI has become more skewed and peaked. These changes in symmetric characteristics of ENSO are reported to be a reflection of the non-linearity of the tropical Pacific system (Hannachi, Stephenson, & Sperber, 2003).

Figure 2 shows the explanatory data analysis before and after 1975. The normal histograms (Fig. 2a) and quantile-quantile plots (Fig. 2b) reveal a change in the lower tail of the SOI after 1975 where extreme El Niño events are observed for the second period. The Jarque-Bera test for normality

(results not shown) indicates that the null hypothesis of normality cannot be rejected for the first period, whereas it can be strongly rejected for the second period. This suggests that extreme negative values (El Niño events) have an effect on the asymmetry, or the non-normality, of the SOI frequency distribution in the second period.

The autocorrelation function (ACF) of the SOI (Fig. 2c) suggests there is no difference between the two periods, whereas the ACF for the squared or the unconditional variance of the SOI (Fig. 2d) shows a change in the ACF in the second period. Figure 2d shows that the autocorrelation coefficients at lag times $k = 1$ and $k = 2$ are higher for the second period than for the first period. This suggests that the time-varying variance or the conditional variance became stronger after 1975. Finally, the monthly SOI box plots (Fig. 2e) reveal no significant change in the monthly variation in the SOI after 1975, except for January and February. Extreme El Niño events are observed in January and February in the second period while the extreme events in the first period are observed during summer.

Although the graphical methods and descriptive statistics indicate changes in SOI characteristics in recent years, the nonparametric tests (Wilcoxon, Levene, and KS tests) are also applied to test the validity of the explanatory analysis for the statistical features of the SOI time series. The results of the nonparametric tests are given in Table 2. The Wilcoxon test shows a strong difference (significant at the 1% level) in the mean value of the SOI before and after 1975. The standard deviation of the SOI shows a slight change at the 5% significance level according to the Levene test. Finally, the nonparametric KS test reveals a significant change in the distribution function of the SOI after 1975 at the 5% significance level.

The stationarity and non-linearity of the SOI time series before and after the change point are evaluated using the ADF and BDS tests. The results are presented in Table 3. The ADF statistics indicate both SOI time series are stationary, and we cannot reject the stationarity at the 1% significance level. The more negative ADF statistic indicates a stronger rejection of the hypothesis of a unit root. Therefore, one can see that the stationarity of the SOI time series for 1976–2011 is less than that for 1940–75. In addition, the results of the BDS test also reveal increasing non-linearity after 1975. For all dimensions ($m1$–$m5$), the non-linearity is significant for both periods, but the test statistics are larger for the second period, which implies the existence of a higher degree of non-linearity in the SOI time series after 1975.

c *ARMA and ARMA-GARCH Error Models for the SOI Time Series*

The parameters of the ARMA models for two SOI time series, 1940–75 and 1976–2011, are given in Table 4. The ARMA (1,1) model is selected based on the minimum Akaike Information Criterion (AIC) in favour of higher order ARMA models.

The p-values of the Engle's test results for the ARCH effect (Fig. 3) indicates that there is no ARCH effect in the residuals of the ARMA(1,1) model for the first segment of the SOI time series, 1940–75, because none of the p-values falls below the critical $p = 0.05$ threshold. On the other hand, it is observed that the first p-value of the test (at lag $k = 1$) for the second SOI time series, 1976–2011, is less than the critical value. This implies that the null hypothesis of no ARCH effect in the residuals of the ARMA(1,1) model for the second SOI time series is rejected. Therefore, it is clear that the time-varying variance, or the heteroscedasticity, appears in the residuals of the ARMA model after 1975. To remove this heteroscedasticity, a GARCH model is fitted to the residuals of the ARMA model to obtain an ARMA-GARCH error model. Therefore, we have an ARMA-ARCH model for the second period of the SOI time series. The parameters of the ARMA-ARCH error model for the second period of the SOI are given in Table 4. It can be seen that the ARCH parameter (α) is statistically significant, whereas the GARCH parameter (β) is not statistically significant and can be eliminated from the model. This implies the rising of a heteroscedasticity in

Table 2. Nonparametric test results for the change in mean, variance, and distribution function.

SOI Series	Wilcoxon	Levene	Kolmogorov-Smirnov
Statistic	−2.62	4.03	1.48
p-value	0.009*	0.04**	0.024**

*Significant at the 1% level.
**Significant at the 5% level.

Table 4. ARMA and ARMA-ARCH models for the SOI time series (p-values of t-statistics for each parameter are given in parentheses).

SOI Series	φ	θ	α	β
1940–1975	0.89 (0.001)	−0.50 (0.001)	—	—
1976–2011	0.87 (0.001)	−0.39 (0.001)	0.25 (0.001)	0.03 (0.82)

Table 3. Stationarity and non-linearity test results for the SOI.

			BDS							
	ADF		1940–1975				1976–2011			
Test	1940–1975	1976–2011	$m2$	$m3$	$m4$	$m5$	$m2$	$m3$	$m4$	$m5$
Statistic	−6.21	−5.61	0.05	0.08	0.10	0.11	0.06	0.11	0.13	0.14
p-value	0.001	0.001	0.001	0.001	0.001	0.001	0.001	0.001	0.001	0.001

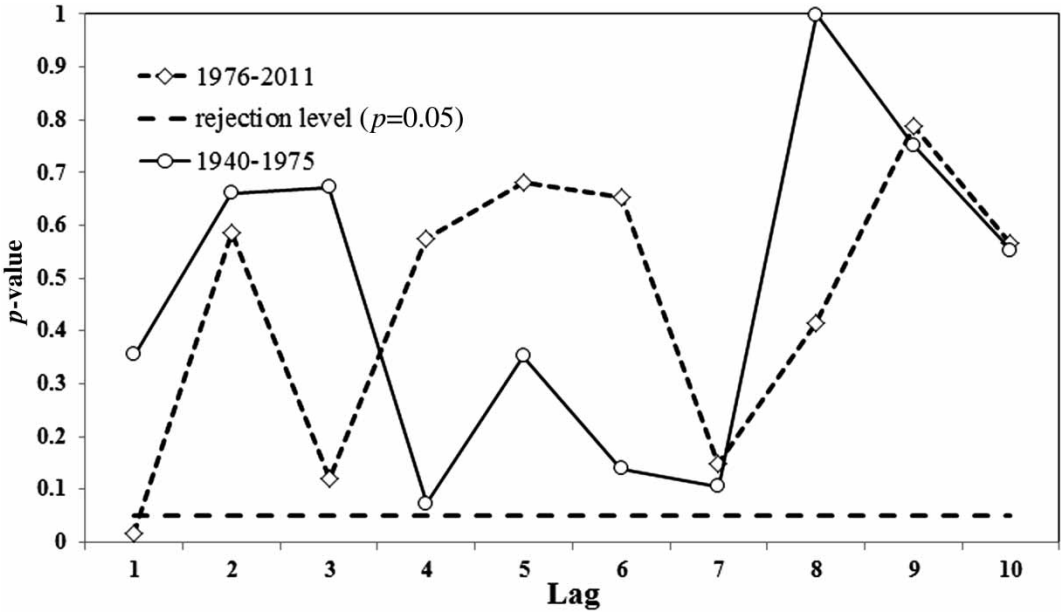

Fig. 3 The *p*-values for Engle's test for the ARMA models.

the residuals, white noise or innovations, of the SOI in recent decades. However, the intensity of the persistence ($\alpha+\beta$) of the volatility does not seem to be very strong ($\alpha+\beta=0.25$).

d *GARCH Models for SOI*

To investigate the ARCH effect in the residuals of an ARMA model, we fitted a GARCH model to the SOI time series before and after 1975 to evaluate the change in the heteroscedastic features of the SOI. The parameters of the GARCH model for the SOI time series (Table 5) are statistically significant for both periods. The GARCH (1,1) model was selected based on the minimum AIC in favour of higher order models.

The model parameters suggest a significant change in the short-run persistence characteristic of the SOI after 1975 when the ARCH parameter increased from 0.29 to 0.43. The degree of long-run persistence shows a reduction from 0.43 to 0.32, and the intensity of persistence, $\alpha+\beta$, increased slightly. It can be seen that the degree of variability (volatility) of the SOI has increased while the memory of the second-order moment of the SOI has decreased as a result of a reduction in β. In other words, the dependence of the SOI variance at each time step on the variances at previous time steps decreased, and the degree of instability (volatility) of the variance increased during recent decades. The conditional variances of the SOI time series are illustrated in Fig. 4, and the monthly distribution of conditional variance is shown in a box plot illustration (Fig. 5).

The conditional variance time series (Fig. 4) is two to three times larger in the second period, especially in 1982–83 when an unprecedented ENSO event occurred. Although the monthly average of the conditional variance remains around one for both periods (Fig. 4), the extreme values of the conditional variance show a remarkable increase in the second period.

Table 5. GARCH models for the SOI time series (*p*-values of *t*-statistics for each parameter are given in parentheses).

SOI Series	ω	α	β	$\alpha+\beta$
1940–1975	0.28 (0.007)	0.29 (0.007)	0.43 (0.008)	0.72
1976–2011	0.33 (0.001)	0.43 (0.001)	0.32 (0.008)	0.75

Extreme heteroscedasticities (outside $\pm 2.7\sigma$) are observed in both periods, but the number of extreme hetereoscedasticities increased in the second period in winter and autumn and decreased in summer. This seasonal shift in the conditional variance can also be detected using the quantile-quantile plot of heteroscedasticity (Fig. 6). If the conditional variances before and after 1975 have the same distribution function, the points should fall approximately along the 45-degree reference line. The greater the departure from the reference line, the greater the evidence that the two conditional variances have different distribution functions.

Apart from December, September, and November, all other months show a remarkable departure from the reference line. The upper tail of the quantile function of heteroscedasticity departs from the 45-degree reference line in most months, but the change in the lower parts (quantiles) is not significant. It is observed that this departure tends to move above the 45-degree reference line after 1975 in January to April (and also in October) and to move below the 45-degree reference line from May to August. This implies a seasonal shift in the extreme volatility of the SOI from summer to winter after 1975.

Finally, in Table 6, the stationarity and non-linearity of the conditional variance of the SOI are presented. From the ADF

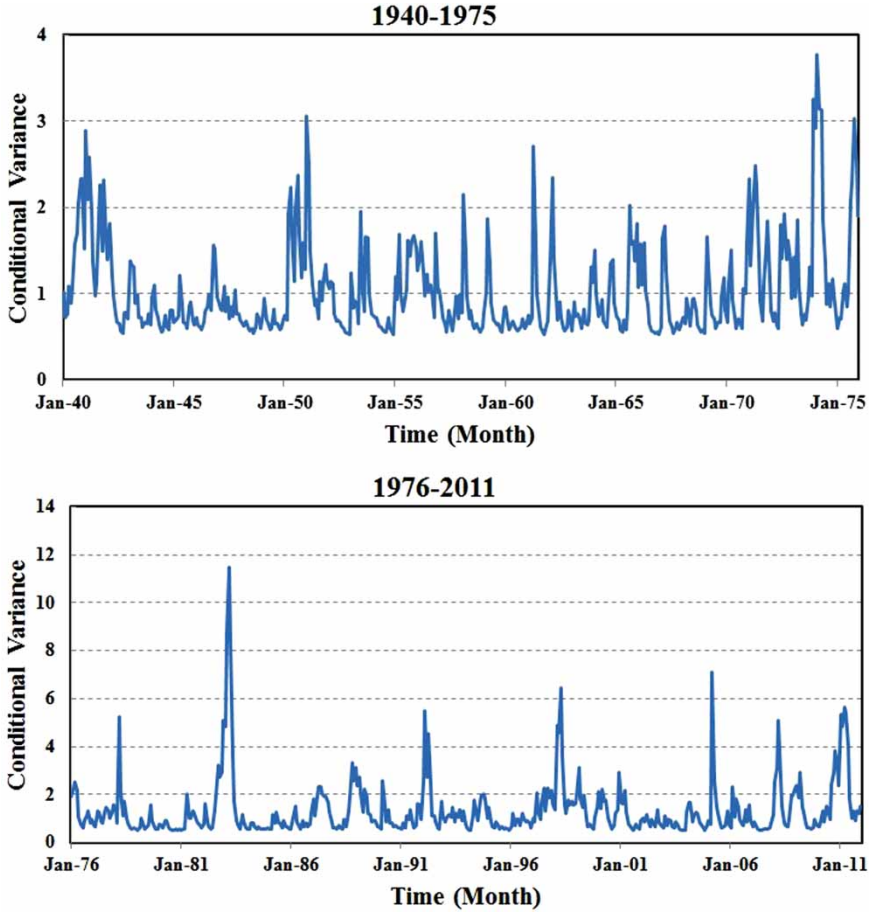

Fig. 4 Conditional variance time series (top panel) before and (bottom panel) after the change point in 1975.

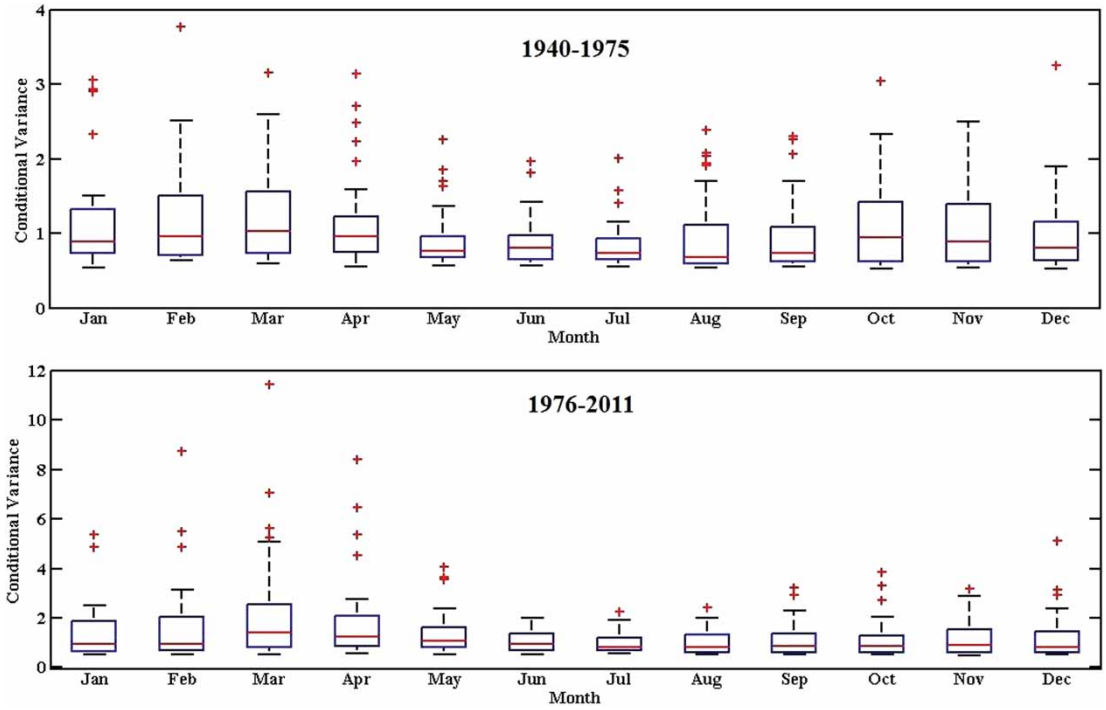

Fig. 5 Box plot for the monthly conditional variance of the SOI before (top panel) and after (bottom panel) the change point in 1975.

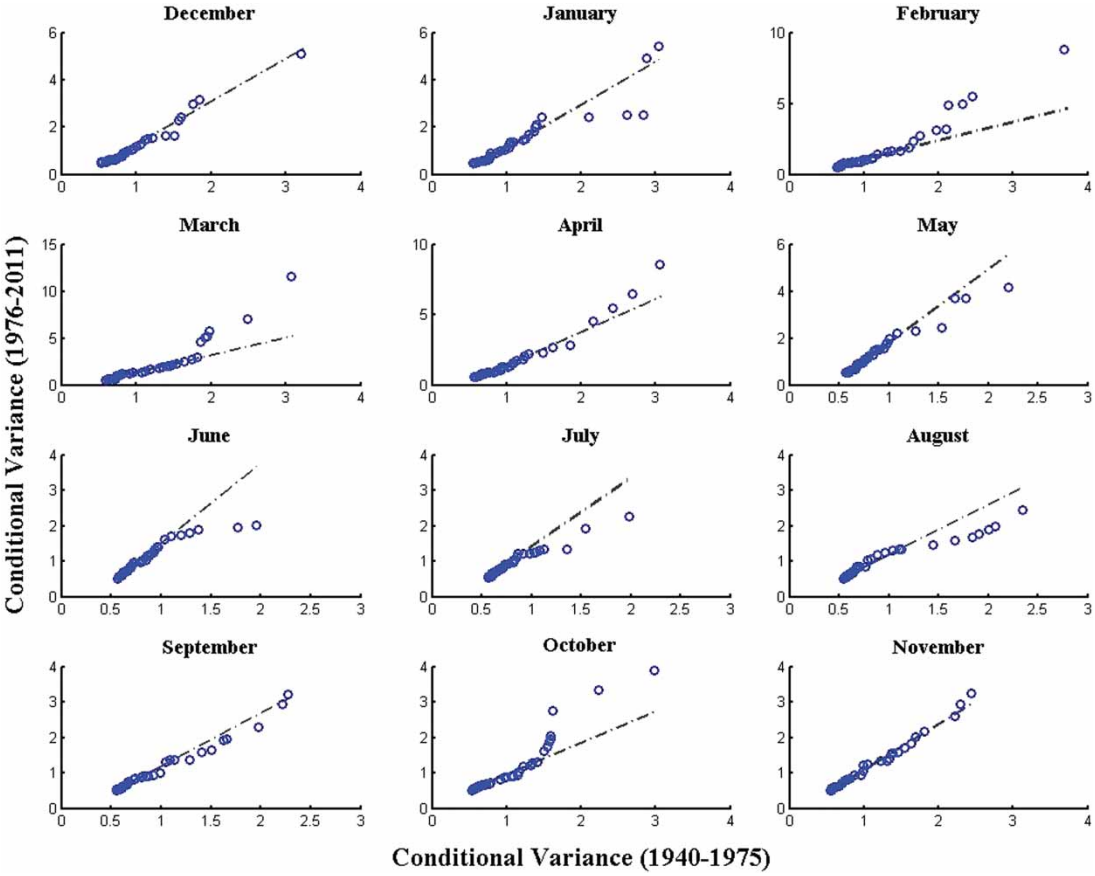

Fig. 6 Monthly quantile-quantile plots for the conditional variances before (*x*-axis) and after (*y*-axis) 1975.

Table 6. Stationarity and non-linearity test results for conditional variance.

	ADF		BDS							
			1940–1975				1976–2011			
Test	1940–1975	1976–2011	*m*2	*m*3	*m*4	*m*5	*m*2	*m*3	*m*4	*m*5
Statistic	−8.73	−7.77	0.08	0.13	0.16	0.17	0.10	0.16	0.20	0.22
p-value	0.001	0.001	0.001	0.001	0.001	0.001	0.001	0.001	0.001	0.001

test results, the stationarity of the conditional variance is clear whereas the level of stationarity for the second period is lower than that for the first period. Moreover, the conditional variance in both periods demonstrates non-linearity, but the degree of non-linearity is higher for the second period. These results indicate a notable change in the second-order moment of the SOI toward more instability, variability, and non-linearity in recent decades.

4 Summary and conclusions

In this paper, the conditional variance or volatility of ENSO is tested and modelled and its changes in recent decades are explored for the first time. Using a Bayesian change point method, a significant change point was detected in 1975. Comparison of the SOI time series before and after 1975 shows a remarkable change in the descriptive statistics, stationarity, and non-linearity of the SOI time series after the change point in 1975. It has been shown that the mean and (unconditional) variance of the SOI increased, and the distribution of the SOI became non-normal and skewed with higher peakedness (coefficient of kurtosis) after 1975. It was also observed that the SOI became less stationary and more non-linear after 1975. The major reason for becoming more asymmetric seems to be a result of the occurrence of more (negative) extreme events after 1975.

The heteroscedasticity was not significant in the residuals of the ARMA model for the first period (1940–75), but it was significant in the residuals of the model after the change point. It has also been observed that the volatility of the SOI has

increased both in the magnitude and frequency of extreme volatilities. The GARCH parameters indicated an increase in the volatility and a decrease in the memory of the SOI variance. This increase in the volatility and second-order moment may lead to an increasing frequency of extreme events such as extreme precipitation and temperature (Arblaster & Alexander, 2012; Higgins, Kousky, & Xie, 2011) or extreme drought conditions (Baling & Goodrich, 2007; Rajagopalan, Cook, Lall, & Ray, 2000) in relation to extreme ENSO phases. These changes may also lead to an increase in ENSO-driven climate uncertainty and variability and may make future climate prediction extremely difficult at both regional and global levels (Tang & Deng, 2010).

5 Possible future work

It would be very interesting to investigate the effect of the change in ENSO volatility on the change in El Niño and La Niña phases separately using asymmetric GARCH models. It is also recommended that these models be used to test the volatility of other elements of the tropical ocean–atmosphere system in future studies so that the source of the volatility changes and feedbacks can be determined. It would be interesting to investigate the ability of the ensemble global climate models to simulate and project future changes in ENSO volatility. The seasonal shift in extreme ENSO conditions and the shift in the seasonal volatility are also interesting topics for future studies. In future studies, it is also strongly recommended to use long ENSO time series to investigate the change in volatility across centuries and decades.

Acknowledgements

The authors would like to thank the Natural Sciences and Engineering Research Council (NSERC) of Canada and the Canada Research Chairs (CRC) program for financial support.

References

Ahn, J. H., & Kim, H. S. (2005). Nonlinear modeling of El Niño/Southern Oscillation Index. *Journal of Hydrologic Engineering*, *10*, 8–15.

An, S. I., & Wang, B. (2000). Interdecadal change of the structure of the ENSO mode and its impact on the ENSO frequency. *Journal of Climate*, *13*, 2044–2055.

Arblaster, J. M., & Alexander, L. V. (2012). The impact of the El Niño-Southern Oscillation on maximum temperature extremes. *Geophysical Research Letters*, *39*, L20702. doi:10.1029/2012GL053409

Baling, R. C., & Goodrich, G. B. (2007). Analysis of drought determinants for the Colorado River basin. *Climatic Change*, *82*, 179–194.

Bollerslev, T. (1986). Generalized autoregressive conditional heteroscedasticity. *Journal of Econometrics*, *31*, 307–327.

Boucharel, J., Dewitte, B., du Penhoat, Y., Garel, B., Yeh, S. W., & Kug, J. S. (2011). ENSO nonlinearity in a warming climate. *Climate Dynamics*, *37*, 2045–2065. doi:10/1007/s00382-011-1119-9

Brock, W. A., Dechert, W. D., Scheinkman, J. A., & LeBaron, B. (1996). A test for independence based on the correlation dimension. *Economic Review*, *15*, 197–235.

Chen, C. C., McCarl, B., & Hill, H. (2002). Agricultural value of ENSO information under alternative phase definition. *Climatic Change*, *54*, 305–325.

Chu, L-F., McAleer, M., & Chen, C-C. (2012) How volatile is ENSO for global greenhouse gas emissions and the global economy? Retrieved from http://eprints.ucm.es/16597/

Chu, P. S., & Katz, R. W. (1985). Modeling and forecasting the Southern Oscillation: A time-domain approach. *Monthly Weather Review*, *113*, 1876–1888.

Cobb, K. M., Westphal, N., Sayani, H. R., Watson, J. T., Di Lorenzo, E., Cheng, H., Edwards, R. L., & Charles, C. D. (2013). Highly variable El Niño-Southern Oscillation throughout the Holocene. *Sceince*, *339*, 67–70.

Conover, W. J. (1999). *Practical nonparametric statistics* (3rd ed.). NY, USA: Wiley.

Dickey, D. A., & Fuller, W. A. (1979). Distribution of the estimators for autoregressive time series with a unit root. *Journal of the American Statistical Association*, *74*, 423–431.

Ehsansazeh, E., Ouarda, T. B. M. J., & Saley, H. M. (2011). A simultaneous analysis of gradual and abrupt changes in Canadian low streamflows. *Hydrological Processes*, *24*, 727–739.

Engle, R. F. (1982). Autoregressive conditional heteroscedasticity with estimates of variance of United Kingdom inflation. *Econometrica*, *50*, 987–1008.

Hall, A. D., Skalin, J., & Teresavirta, T. (2001). A nonlinear time series model of El Niño. *Environmental Modelling & Software*, *16*(2), 139–146.

Hannachi, A., Stephenson, D. B., & Sperber, K. R. (2003). Probability-based methods for quantifying nonlinearity in the ENSO. *Climate Dynamics*, *20*, 241–256. doi:10.1007/s00382-002-0263-7

Higgins, R. W., Kousky, V. E., & Xie, P. (2011). Extreme precipitation events in the south-central United States during May and June 2010: Historical perspective, role of ENSO, and trends. *Journal of Hydrometeorology*, *12*, 1056–1070.

Latif, M., & Keenlyside, N. S. (2009). El Niño/Southern Oscillation response to global warming. *Proceedings of the National Academy of Sciences of the United States of America*, *106*, 20578–20583. doi:10.1073/pnas.0710860105

Modarres, R., & Ouarda, T. B. M. J. (2012). Generalized autoregressive conditional heteroscedasticity modeling of hydrologic time series. *Hydrological Processes*, (in press) doi:10.1002/hyp.9452.

NOAA (National Oceanic and Atmospheric Administration). (2012). Climate Prediction Centre [data]. National Weather Service. Retrieved from http://www.cpc.ncep.noaa.gov/

Philip, S., & van Oldenborgh, G. J. (2009). Significant atmospheric nonlinearities in the ENSO cycle. *Journal of Climate*, *22*, 4014–4028. doi:10.1175/2009JCLI2716.1

Qian, C., Wu, Z., Congbin, F., & Wang, D. (2011). On changing El Niño: A view from time-varying annual cycle, interannual variability, and mean state. *Journal of Climate*, *24*, 6486–6500.

Rajagopalan, B., Cook, E., Lall, U., & Ray, B. K. (2000). Spatiotemporal variability of ENSO and SST teleconnections to summer drought over the United States during the twentieth century. *Journal of Climate*, *13*, 4244–4255.

Robbins, M., Gallagher, C., Lund, R., & Aue, A. (2011). Mean shift testing in correlated data. *Journal of Time Series Analysis*, *32*, 498–511.

Ropelewski, C. F., & Halpert, M. S. (1987). Global and regional scale precipitation patterns associated with the El Niño/Southern Oscillation. *Monthly Weather Review*, *115*, 1606–1626.

Seidou, O., & Ouarda, T. B. M. J. (2007). Recursion-based multiple change point detection in multiple linear regression and application to river streamflows. *Water Resources Research*, *43*, W07404. doi:10.1029/2006WR005021

Shabbar, A., & Khandekar, M. (1996). The impact of El Niño-Southern Oscillation on the temperature field over Canada: Research note. *Atmosphere-Ocean*, *34*, 401–416.

Stahle, D. W. D., Arrigo, R. D., Krusic, P. J., Cleaveland, M. K., Cook, E. R., Allan, R. J., Cole, J. E., Dunbar, R. B., Therrekk, M. D., Gay, D. A., Moore, M. D., Stokes, M. A., Burns, B. T., Villanueva-Diaz, J., & Thompson, L. G. (1998). Experimental dendroclimatic reconstruction of the Southern Oscillation. *Bulletin of the American Meteorological Society*, *79*(10), 2137–2152.

Tang, Y., & Deng, Z. (2010). Low-dimensional nonlinearity of ENSO and its impact on nonlinearity. *Physica D*, *239*, 258–268.

Timmermann, A. (1999). Detecting the nonstationary response of ENSO to greenhouse warming. *Journal of Atmospheric Sciences*, *56*, 2313–2325.

Trenberth, K. E., & Hoar, T. J. (1997). El Niño and climate change. *Geophysical Research Letters*, *24*, 3057–3060.

Wang, F. (2007). Investigating ENSO sensitivity to mean climate in an intermediate model using a novel statistical technique. *Geophysical Research Letters*, *34*. doi:10.1029/2007GL029348

Wang, W. (2006). *Stochasticity, nonlinearity and forecasting of streamflow processes.* Amsterdam: Delft University Press, ISBN 1-58603-621-1.

Wu, Z., Huang, N. E., Long, S. R., & Peng, C.-K. (2007). On the trend, detrending, and variability of nonlinear and nonstationary time series. *Proceedings of the National Academy of Sciences of the United States of America*, *104*, 14889–14894.

Xue, Y., Smith, T. M., & Reynolds, R. W. (2003). Interdecadal changes of 30-yr SST normals during 1871–2000. *Journal of Climate*, *16*, 1601–1612.